THE JOURNAL OF BIOLOGICAL CHEMISTRY VOL. 285, NO. 38, pp. 29434–29445, September 17, 2010
© 2010 by The American Society for Biochemistry and Molecular Biology, Inc. Printed in the U.S.A.

Expression of Slug Is Regulated by c-Myb and Is Required for Invasion and Bone Marrow Homing of Cancer Cells of Different Origin*[S]

Received for publication, November 25, 2009, and in revised form, July 8, 2010 Published, JBC Papers in Press, July 11, 2010, DOI 10.1074/jbc.M109.089045

Barbara Tanno[‡], Fabiola Sesti[‡1], Vincenzo Cesi[‡], Gianluca Bossi[§], Giovanna Ferrari-Amorotti[¶2], Rita Bussolari[‖], Donatella Tirindelli[‡], Bruno Calabretta[¶], and Giuseppe Raschellà[‡3]**

*From the [‡]Italian National Agency for New Technologies, Energy and Sustainable Economic Development (ENEA), Research Center Casaccia, Laboratory of Radiation Biology and Biomedicine, 00123 Rome, Italy, the [§]Regina Elena Cancer Institute, Department of Experimental Oncology, 00158 Rome, Italy, the [¶]Department of Biomedical Sciences, and [‖]Department of Hematology-Oncology, University of Modena, 41100 Modena, Italy, and the **Kimmel Cancer Center, Thomas Jefferson University, Philadelphia, Pennsylvania 19107*

In metastatic cancer cells, the process of invasion is regulated by several transcription factors that induce changes required for migration and resistance to apoptosis. Slug (SNAI2, Snail2) is involved in epithelial mesenchymal transition in physiological and in pathological contexts. We show here that in embryonic kidney, colon carcinoma, chronic myeloid leukemia-blast crisis, and in neuroblastoma cells, expression of Slug is transcriptionally regulated by c-Myb via Myb binding sites in the 5′-flanking region and in the first intron of the *slug* gene. In embryonic kidney and neuroblastoma cells, c-Myb induced vimentin, fibronectin, and N-cadherin expression and membrane ruffling via actin polymerization consistent with the acquisition of a mesenchymal-like phenotype. Furthermore, down-regulation of endogenous c-Myb levels in colon carcinoma cells led to increased expression of E-cadherin and reduced levels of vimentin. Some of these changes are predominantly Slug-dependent as Slug silencing via RNA interference (RNAi) reverts the cells to a quasi-parental condition. Changes in gene expression and morphology induced by c-Myb-activated Slug correlated with increased ability to migrate (embryonic kidney) and to invade through a Matrigel membrane (embryonic kidney, colon carcinoma, neuroblastoma). c-Myb-dependent Slug expression was also essential for the homing of chronic myeloid leukemia K562 cells to the bone marrow. In summary, we show here that the proto-oncogene c-Myb controls Slug transcription in tumor cells of different origin. Such a regulatory pathway contributes to the acquisition of invasive properties that are important for the metastatic process.

The main cause of death for cancer patients is metastasis, the formation of secondary tumors in organs distant from the site of the original cancer (1). A series of well coordinated and interconnected biological processes must occur to drive tumor cells from the site of the primary neoplasm to a distant location (2). To acquire an invasive phenotype, tumor cells need to interact with components of the extracellular matrix, such as collagen and hyaluronic acid, and with soluble growth factors, such as members of the transforming growth factor β (TGF-β) and fibroblast growth factor families, epidermal growth factor, and scatter factor/hepatocyte growth factor (3). During local invasion, the first step of the metastatic process, tumor cells of epithelial origin undergo a trans-differentiation process termed epithelial mesenchymal transition (EMT)[4] (3). During EMT, tumor cells lose cell-cell interactions and apico-basal polarity and acquire mesenchymal and migratory properties (4). EMT is a reversible process; once cancer cells localize to a site of metastasis, they undergo a mesenchymal epithelial transition through which they reacquire many of the characteristics of the tumor cells at the primary site (5). In EMT, loss of epithelial properties occurs through down-regulation of the expression of epithelial-specific proteins (*e.g.* E-cadherin and cytokeratins) and the acquisition of mesenchymal proteins (*e.g.* N-cadherin and vimentin) (6). In addition, cancer cells undergoing EMT activate proteinases that allow them to pass through the extracellular matrix and to become more resistant to anoikis, a form of cell death that occurs in cells detached from their stroma support (7). A central question for understanding the process of metastasis at the molecular level is, Which are the regulators of the genes activated or repressed during EMT that occurs at the onset of invasion? Several transcription factors that strongly repress E-cadherin (such as members of the Snail, ZEB, and basic helix-loop-helix (bHLH) families) are now thought to be inducers of the phenotypic changes required for EMT (4). Nevertheless, the specific role of these different repressors in tumorigenesis is not fully understood. In particular, the Snail family of transcription factors that in vertebrates includes Snail (SNAI1, Snail1), Slug (SNAI2, Snail2), and SNAI3, is involved in

* This work was supported in part by the Fondazione Italiana per la Lotta al Neuroblastoma (to G. R.). This work was also supported by National Institutes of Health Grant RO1 CA95111 (NCI; to B. C.) and Associazione Italiana per la Ricerca sul Cancro IG Grant 8804 (to G. B.).

[S] The on-line version of this article (available at http://www.jbc.org) contains supplemental Fig. S1.

[1] Supported by a research contract from the Fondazione Italiana per la Lotta al Neuroblastoma.

[2] Supported by a fellowship of the Associazione Italiana per la Ricerca sul Cancro.

[3] To whom correspondence should be addressed: ENEA Research Center Casaccia, Laboratory of Radiation Biology and Biomedicine, Via Anguillarese, 301, 00123 Rome, Italy. Tel.: 39-0630483172; Fax: 39-0630486559; E-mail: giuseppe.raschella@enea.it.

[4] The abbreviations used are: EMT, epithelial mesenchymal transition; DOX, doxycycline; MBS, Myb binding sites.

This is an Open Access article under the CC BY license.

physiological (8) and pathological (9, 10) EMT. Snail is expressed during mesoderm formation, gastrulation and neural crest development and in the majority of developmental processes in which EMT occurs (for review, see Ref. 4). Slug expression has been detected in mesoderm and migratory neural crest cells as well as in other tissues not always associated with EMT (for review, see Ref. 4). Slug contributes to invasion in melanomas (11) and in malignant mesotheliomas, where it is induced by stem cell factor (12). We have recently demonstrated that Slug silencing inhibits neuroblastoma invasion *in vitro* and *in vivo* (13). Also Snai1 expression appears to be correlated with invasive growth potential in human cancer (14). Both Snail and Slug are zinc finger transcription factors that share a common organization (4). In most cases they act as transcriptional repressors through a conserved domain (the SNAG domain) located in the N terminus of the protein (4). Several direct and indirect targets of Snail genes are associated with survival, proliferation, cell shape, and motility (8). However, knowledge of the mechanisms that control Snail and Slug expression is incomplete.

The c-Myb proto-oncogene is a transcription factor involved in leukemogenesis in several species including humans (15). It can be activated by overexpression or inappropriate expression, structural alteration, and/or genomic rearrangements and is required in the bone marrow, colonic crypt, and neurogenic niches as indicated by the phenotype of global or tissue-specific knock-out mice (for review, see Ref. 15). Abnormal c-Myb expression has been demonstrated in colon (16, 17) and breast carcinomas (18, 19). We have previously shown that c-Myb is expressed also in neuroblastoma cell lines and primary tumors (20, 21). Of interest, simultaneous expression of c-Myb and Slug was detected in delaminating neuroblasts of the avian embryonic neural crest (22). In this context, c-Myb is necessary for the motile phenotype as demonstrated by analysis of the effects of c-Myb knockdown induced by morpholino oligos (22).

We show here that c-Myb activates Slug expression through a transcriptional mechanism in embryonic kidney, colon carcinoma, chronic myeloid leukemia, and neuroblastoma cells. c-Myb-activated Slug expression is associated with increased *in vitro* invasion and the acquisition of mesenchymal markers and is required for bone marrow homing of K562 cells in mice. Together, these data support the existence of a functional relationship between the proto-oncogene *c-myb* and metastasis-associated *slug* in hematopoietic and non-hematopoietic cancer cells.

EXPERIMENTAL PROCEDURES

Cell Lines—LAN-5 (human neuroblastoma) (20), HEK-293 (human embryonic kidney cells transformed by adenovirus type 5 DNA) (23), and LoVo (human colon carcinoma) (24) cells were cultured in DMEM medium (Euroclone), COLO-205 (human colon carcinoma) (16) were cultured in RPMI 1640 medium (Euroclone), and K562 (chronic myeloid leukemia) (25) cells were cultured in Iscove's modified Dulbecco's medium (Euroclone) supplemented with 10% FCS at 37 °C, 5% CO_2 in 100% humidity.

Plasmids—Regulatory regions of the human *slug* gene were cloned into pGL3 Basic (Slug prom) and pGL3 Promoter (intron 1 and intron 2) vectors (Promega, Madison, WI) after PCR amplification of the corresponding genomic regions with the Pfu enzyme (Promega) using these primers: *Slug* prom forward, 5′-GTT GGC TGG TAC CGC TCC TGC GCC CCT C-3′; *slug prom* reverse, 5′GAA GGA AAG ATC TCT TGC CAG CGG GTC TGG-3′; *slug* intron 1 forward, 5′-GTT GGC TGG TAC CGT AAA AAG AGA AAA ATA TAT CTA GAA CTA CGT-3′; *slug* intron 1 reverse, 5′-GAA GGA AAG ATC TCT GGG AAA GAA AAG GGA GGG AG-3′; *Slug* intron 2 forward, 5′-GTT GGC TGG TAC CGT AAG AGA AAA ACC ATA GGC AGG-3′; *slug* intron 2 reverse, 5′-GAA GGA AAG ATC TCT GGG GGT GGA GTG GGA G-3′.

The PCR-amplified products were digested with KpnI/BglII restriction enzymes and cloned into pGL3 vectors using standard cloning procedures. The sequence of each construct was verified by dideoxy sequencing. The mutants in A, B, C, and D sites and the double mutant A/B were obtained by using the QuikChange site-directed mutagenesis kit (Stratagene, La Jolla, CA) according to the manufacturer's instructions.

The primers used were: *slug* prom A forward, 5′-CCC TCC CAG CCA AGA TGA GCT CAG TGC GTA AAG GAG CC-3′; *slug* prom A reverse, 5′-GGC TCC TTT ACG CAC TGA GCT CAT CTT GGC TGG GAG GG-3′; Slug prom B forward, 5′CCC GCC GGA TCC TGA TCC GCG CCG GGC-3′; Slug prom B reverse, 5′-GCC CGG CGC GGA TCA GGA TCC GGC GGG-3′; Slug int1 C forward- 5′-GAG CCA AAG ATT CAA ATA TGT TCC TTT TTA ACA GTG TCC TG-3′; Slug int1 C reverse, 5′-CAG GAC ACT GTT AAA AAG GAA CAT ATT TGA ATC TTT GGC-3′; Slug int2 D forward, 5′-GTT CTG TGA GAT TAC CCC CAG TAAT C-3′; Slug, int2 D reverse, 5′-GAT TAC TGG GGG TAA TCT CAC AGA AC-3′.

Luciferase Assays, Transfections, and Infections—For luciferase assays cells were co-transfected with wild type or mutated reporter plasmids and pcDNA3-c-Myb or the empty vector pcDNA3 using Lipofectamine 2000 (Invitrogen) according to the manufacturer's instructions. Luciferase assays were performed 36 h later using a detection kit (PerkinElmer Life Sciences).

Stable transfections were carried out by transfecting cells with pcDNA3-c-Myb containing the full-length cDNA for human *c-myb* using Lipofectamine 2000 (Invitrogen). G418 (Sigma) selection (600 – 800 μg/ml) was started 48 h after transfection. Mixed populations were expanded for 14–21 days and tested for c-Myb expression.

For transient RNAi, HEK-293 cells were transfected with a validated pool of four siRNAs directed to different segments of the c-Myb mRNA coding sequence (MYB ON-TARGETplus SMARTpool, Dharmacon, Thermo Fisher Scientific, Waltham, MA) alone or in combination with the Halo-c-Myb expression vector using Lipofectamine 2000 (Invitrogen) according to the manufacturer's instructions. Control transfections were carried out with a pool of validated siRNA controls (Dharmacon).

For shRNA-mediated inhibition of Slug, we used lentiviral vector pLKO-Slug3 (Addgene, Cambridge, MA) which encodes an shRNA directed against human Slug (11). In control infections, we used lentiviral vector pLKO-GFP that encodes an

shRNA directed against GFP (11). For shRNA-mediated c-Myb inhibition we used vector pLVsh-c-Myb (26).

Lentiviruses were generated by transient co-transfection of DNA into 293FT cells. Briefly, 2.5×10^6 293FT cells were seeded in 10-cm plates and cotransfected with 21 μg of appropriate packaging plasmids pCMVd8.2:pCMV-VSVG (2.5:1) and 20 μg of pLKO-*SLUG* or pLKO-GFP vectors using a calcium phosphate transfection kit (Invitrogen). After 6–8 h, medium was replaced with 6.0 ml of complete medium supplemented with 1.0 mM of sodium pyruvate (Sigma). Lentiviral stocks were harvested 48 h later, centrifuged 5 min at 3000 rpm, aliquoted, and stored at −80 °C. When needed, viral supernatants were supplemented with 8 μg/ml Polybrene (Sigma) and used to infect indicated tumor cell lines; 18 h after infection, lentivirus-transduced cells were selected with puromycin (2–3 μM; Sigma) or by flow cytometric sorting of GFP-positive cells. The human *slug* retroviral vector was generated by cloning the full-length cDNA of human *slug* obtained by reverse transcriptase-PCR into the pBABE-puro vector system using standard techniques. Slug sequence was confirmed by dideoxysequencing.

Infectious retroviruses were obtained by transient cotransfection of vector DNA into amphotropic Phoenix cells. Briefly, 4×10^6 cells were seeded in 10-cm plates, and the plates were cotransfected with 1.5 μg of packaging plasmid pCMV-VSVG and 13.5 μg of pBABE-Slug or pBabe-puro vector by calcium phosphate precipitation. Transfection was carried out in the presence of 25 μM chloroquine (Sigma). Viral supernatants were harvested 24 h post-transfection by centrifugation at 3000 rpm for 5 min, supplemented with 5 μg/ml Polybrene (Sigma) before infection, and used to infect K562 cells. Forty-eight hours after infection, cells were selected by puromycin (Sigma).

Western Blotting—Whole cell proteins were extracted from parental and derivative cell lines and separated on SDS-polyacrylamide gels, and Western blot analyses were carried out as previously described (27). Antibodies used were anti-c-Myb (clone 1–1) from Millipore (Temecula, CA), anti-Snail (AB 17732) from Abcam (Cambridge, UK), anti-Slug (G-18), anti-p53 (DO-1), anti-Bcl-2 (N-19), and anti-Bax (N-20), all from Santa Cruz Biotechnology (Santa Cruz, CA), anti-Vimentin (V9) from Sigma, anti-fibronectin, anti-E-cadherin, and anti-N-cadherin, all from BD Transduction Laboratories, and anti-β-actin (AC-15) from Sigma.

Immunofluorescence—Cells were seeded at $3.5 \times 10^4/\text{cm}^2$ and transfected with HaloTag® pHT2 vector and pHT2 c-Myb vector (Promega) utilizing TransFast™ transfection reagent (Promega). After 24 h, cells were labeled with HaloTag® TMR (Promega) as recommended by the manufacturer. After HaloTag® ligand labeling of live cells, fixation was carried out by paraformaldehyde. Immunocytochemistry was performed according to standard procedures. Primary antibodies were anti-Slug (G-18; Santa Cruz Biotechnology) and anti-E-cadherin and anti-N-cadherin (BD Transduction Laboratories). Secondary antibody was anti-goat (Alexa Fluor 488) (Molecular Probes, Eugene, OR). Alexafluor 488 Phalloidin from Molecular Probes (Invitrogen) was utilized according to manufacturer's instructions.

Chromatin Immunoprecipitation—15×10^6 cells were seeded and transfected with HaloTag® pHT2 *c-myb* vector (Promega) utilizing TransFast™ Transfection Reagent (Promega). Cross-linking was performed 24 h post-transfection. HaloCHIP™ was carried out according to the manufacturer's instructions (HaloCHIP™ System, Promega).

Primers used for amplification of the regions including the potential Myb binding sites were: A forward, 5′-CTG AAC CTC TCA GCT GTG ATT GG-3′; A reverse, 5′-CTT TAC GAA CTG AGC CCG TTT T-3′; B forward, 5′-CCG CAC CTG AGC ACG G-3′; B reverse, 5′-CGC GGA TAA CGG TCC G-3′; C forward, 5′-CGT ATC TAG AGC TTT GCA AAT ATG AAT C-3′; C reverse, 5′-TTC AGG ACA CTG TTA AAA AGG AAA AC-3′; D forward, 5′-AAA ACC ATA GGC AGG AAT GTT ACT CT-3′; D reverse, 5′-AGC ACT ATG TCA CAA CTT CAT GCA-3′; adenosine deaminase forward, 5′-CTC CTC CTT TTT GTC TTC CT-3′; adenosine deaminase reverse, 5′-GAA ACT CAG TCT CCT TTG TTC CCC-3′.

For ChIP experiments performed in K562 cells, samples were prepared as described previously (28). Immunoprecipitations were carried out using 6 μg of anti-c-Myb (clone 1-1 from Millipore), anti-p53 (DO-1 from Santa Cruz), or no antibody. Recovered DNA was analyzed by real-time quantitative PCR. For every promoter fragment analyzed, each sample was quantified in triplicate from two independent immunoprecipitations. The relative proportions of immunoprecipitated promoter fragments were determined by a relative quantification method; a standard curve was generated with serial dilution of the input sample and used as a reference standard for extrapolating quantitative information for ChIP sample. Relative enrichment was calculated as follows: relative enrichment = $x - y$, where x = quantity of sample/quantity of input, and y = quantity of control (immunoprecipitation with unrelated antibody)/quantity of input. Primers were the same as those utilized for semiquantitative PCR analysis. Real-time PCR was carried out using SYBR Green PCR Master Mix (Applied Biosystems, Foster City, CA) in an ABI PRISM® 7000 Sequence Detection System (Applied Biosystems) according to the manufacturer's instructions.

Flow Cytometric Analysis—1×10^6 cells were harvested, and the pellets were washed twice with PBS. Cells were then fixed in cold 70% ethanol added drop-wise while vortexing gently. Fixed cells were kept overnight at 4 °C. Cells were centrifuged, and pellets were resuspended in 1 ml of PI/RNase staining buffer (BD Biosciences). Reactions were incubated for 20 min at 4 °C, protected from the light. Samples were analyzed by flow cytometry using a FACSCalibur flow cytometer (BD Biosciences). For each sample, at least 2×10^4 cells were analyzed. Cell cycle distribution and hypodiploid DNA content were calculated by Cell Quest software (BD Biosciences). Statistical significance (p) was calculated by two-tailed Student's t test.

Migration and Invasion Assays—Wound healing assay (29) was carried out by plating cells to confluence. Cell surface was scratched using a pipette tip. Cells were allowed to repopulate the scratched area for 3 days, and photographs were taken using a digital camera mounted on an inverted microscope. For migration and invasion assays, cells were plated (1.25×10^5 cell/well) in the BD migration or Matrigel®-coated invasion

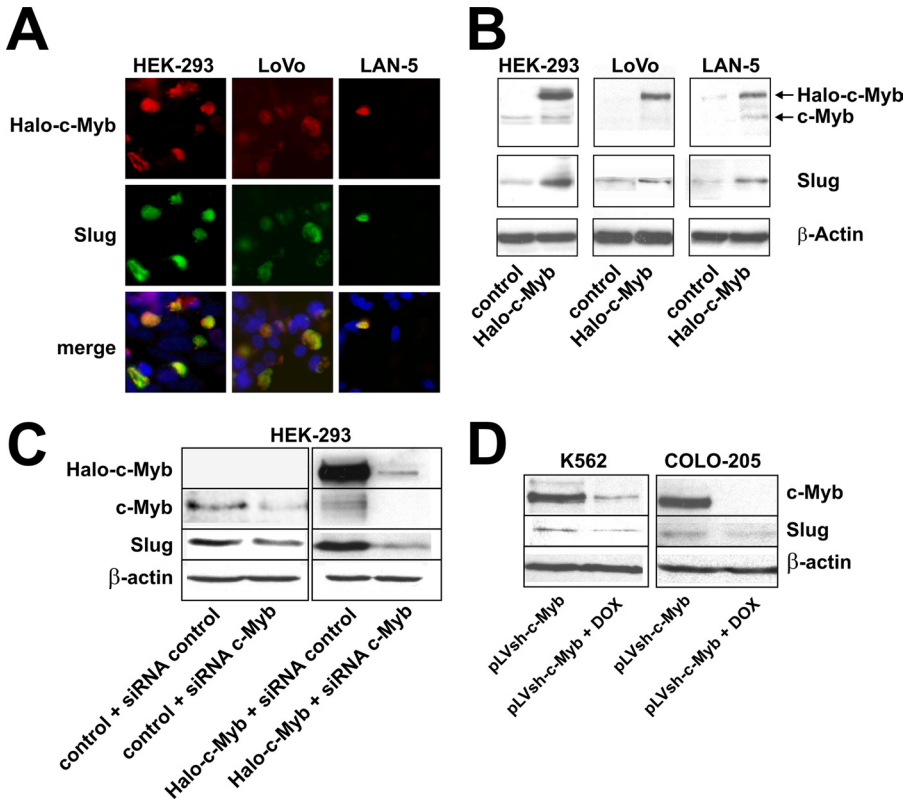

FIGURE 1. *A*, cell lines (indicated on the *top of the panels*) were transfected with a plasmid encoding Halo-c-Myb. Halo-c-Myb protein was detected with red fluorescent Halo peptide (see "Experimental Procedures"). In the same cells Slug was detected with anti-Slug antibody (*green*). In the merge panels, nuclear staining of Halo-c-Myb and Slug in the same nuclei is *yellow*. Nuclei were counterstained by DAPI. Original magnification is 100×. *B*, shown is Western blot analysis of c-Myb and Slug expression in cell lines (indicated on the *top of the panels*) transfected with Halo-c-Myb plasmid. In the *top panels*, Halo-c-Myb and endogenous c-Myb (c-Myb) are indicated by *arrows*. Anti-β-actin Western blotting was used to normalize protein loading. *C*, Western blot analysis of HEK-293 cells co-transfected with empty vector (*control*) and scramble (*siRNA control*) or c-Myb (*siRNA c-Myb*) siRNA or co-transfected with Halo-c-Myb vector (*Halo-c-Myb*) and control or c-Myb siRNAs is shown. *D*, Western blot analysis of c-Myb and Slug expression in COLO-205 and K562 cells infected with doxycycline-inducible pLVsh-c-Myb lentiviral vector expressing an shRNA directed against c-Myb is shown. DOX treatment was 7.5 μg/ml for 24 h. β-Actin was detected for normalization.

chambers (BD Biosciences). Medium in the upper chamber was supplemented with 2% heat-inactivated FCS. In the lower chamber FCS concentration was 20%. After 24 h, cells migrated into the lower chamber were stained and counted. Experiments were carried out in triplicate and repeated twice.

Homing Assay of K562 Cells in SCID Mice—For the homing assay, NOD/SCID mice (NOD.CB17-Prkdc ^{scid}/J, Charles River Laboratories International, Inc. Wilmington, MA) (three/group) were treated with doxycycline in the drinking water (2 mg/ml; 72 h) before injection (2.5×10^6 cells/mouse) with untreated or doxycycline (DOX)-treated (36 h, 7.5 μg/ml) K562 cells (c-MybshRNA or c-MybshRNA/full-length Slug). 24 h after injection, mice were sacrificed, bone marrow was harvested, and the number of K562 cells was determined by GFP positivity and by methylcellulose colony formation assays of marrow cells plated in the absence of hemopoietic cytokines to allow only growth of K562 cells.

RESULTS

c-Myb Induces Slug Expression—Human cell lines LAN-5 (neuroblastoma) (20), LoVo (colon carcinoma) (24), and HEK-293 (embryonic kidney cells) (23) were transfected with an expression vector encoding c-Myb in frame with an Halo-Tag that binds with high affinity to a red-fluorescent peptide (Halo peptide, see "Experimental Procedures"). Transfected cells were treated with the Halo peptide and subsequently processed for immunodetection of Slug using a specific antibody. Red fluorescence from the Halo peptide bound to the c-Myb protein and green fluorescence from Slug co-localized in the same nuclei of transfected cells (Fig. 1*A*).We also compared the level of expression of c-Myb and Slug in c-Myb- and in empty vector-transfected cells. As shown in Fig. 1*B*, ectopic expression of c-Myb was associated with increased Slug levels. To assess whether Slug expression was controlled by c-Myb, HEK-293 cells were transfected with a c-Myb siRNA pool of four different siRNAs validated to produce minimal off-target effects (see "Experimental Procedures") or with a control pool (four different control siRNAs) in the presence or in the absence of an expression vector encoding Halo-tagged c-Myb. Forty-eight hours after transfection, protein extracts were prepared, and Western blots were carried out to detect c-Myb and Slug. Compared with cells transfected with control siRNAs, c-Myb and Slug expression were decreased in cells transfected with the siRNA pool targeting c-Myb (~60% in cells that had only endogenous c-Myb and essentially undetectable in cells with ectopic expression of Halo-c-Myb) (Fig. 1*C*). In addition, colon carcinoma COLO-205 (16) and chronic myeloid leukemia K562 cells (25) that express high levels of endogenous c-Myb were infected with a dicistronic lentiviral vector encoding a DOX-inducible c-Myb shRNA and GFP (pLVsh-c-Myb). Upon DOX treatment (7.5 μg/ml for 24 h), c-Myb and Slug expression were down-regulated (Figs. 1*D*), demonstrating that endogenous c-Myb also controls Slug levels.

c-Myb Induces an Increase of Slug Expression through a Transcriptional Mechanism—To investigate whether the increase in Slug levels induced by c-Myb expression is due to a transcriptional mechanism, we first searched the 5′-flanking (5′ from the initial ATG) and intronic regions of the Slug gene for potential Myb binding sites (MBS). By setting the homology threshold to 86% with the consensus MBS (TFsearch web site), we identified two putative MBS in the 5′-flanking region: (A at nucleotides −9 to −4 and B at nucleotides +122 to +128 from the transcription start site), one in the first intron (C) and one in the second intron (D). A scheme of the human *slug* gene and the

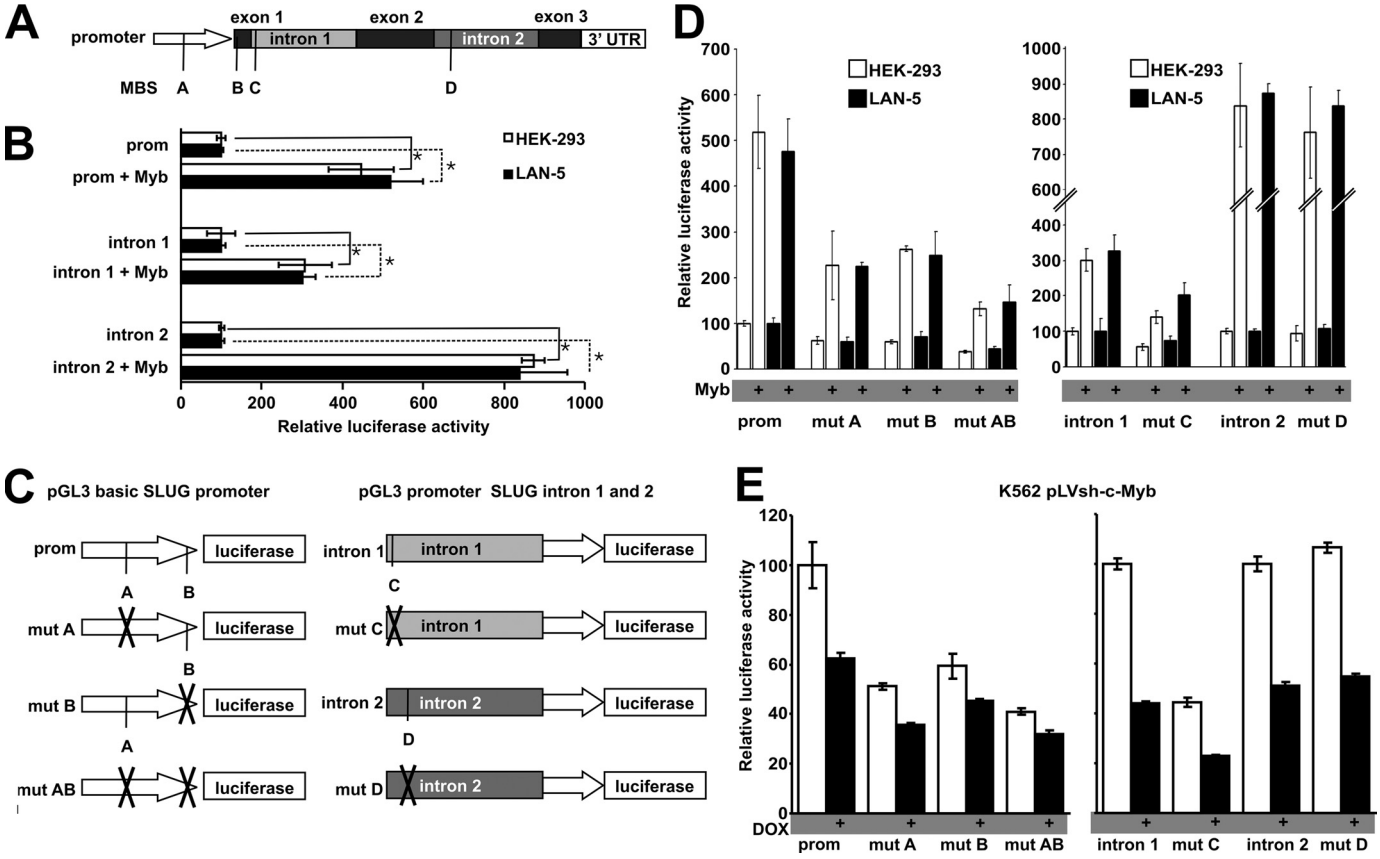

FIGURE 2. *A*, shown is a scheme of the human *slug* gene. Potential Myb binding Sites in the promoter region and in intron 1 and 2 are indicated. *B*, functional assays were carried out by transfection of HEK-293 and LAN-5 cells with luciferase reporter plasmids containing the *slug* promoter (*prom*) or intron 1 or intron 2 alone or with an expression plasmid encoding c-Myb (*Myb*). Transcriptional activity of each reporter plasmid alone was set at 100. *C*, shown is the scheme of *wt* or MBS- mutated reporter plasmids. *D*, *left*, luciferase assays were carried out by co-transfection of HEK-293 and LAN-5 cells with reporter plasmids containing the *wt slug* promoter (*prom*) or the promoter mutated in site A (*mut A*) or in site B (*mut B*) or at both sites (*mut AB*) and an expression vector for c-Myb or the empty vector; *right*, luciferase assays were carried out by co-transfecting reporter plasmids containing *wt* intron 1 or intron 2 or the introns mutated in site C (*mut C*) or in site D (*mut D*) and an expression vector for c-Myb or the empty vector. The difference between the transcription activity of each reporter in the presence of c-Myb compared with that of the same reporter with the empty vector was always statistically significant ($p < 0.05$, two-tailed Student's *t* test) except for reporter mut D, whose transcription activity did not vary in the presence of c-Myb. *E*, luciferase assays were carried out in K562 cells infected with pLVsh-c-Myb by transfection of *wt* and mutated reporter vectors described in *D*. DOX treatment (7.5 μg/ml; 36 h) was started 18 h after transfection. Transcriptional activities of the *wt* reporters (prom, intron 1, and intron 2) cotransfected with the empty vectors were set at 100. Experiments in *B*, *D*, and *E* were carried out twice in triplicate. Values ± S.E. are reported.

position of the potential MBSs is shown in Fig. 2*A*. We cloned a portion of the *slug* 5′-flanking region (−280 to +128 from the transcription start site) in the reporter vector pGL3-basic (hereafter named Slug prom) and intron 1 (744 bp) and 2 (906 bp) in pGL3-promoter vector. Co-transfection of HEK-293 and LAN-5 cells with the reporter vectors containing the *slug* prom or intron 1 and 2 and an expression vector for c-Myb yielded a significant increase in luciferase activity (Fig. 2*B*), demonstrating that Slug transcription is c-Myb-responsive. We assessed the functional relevance of these putative MBS by mutating each site (a scheme of the *wt* and mutant vectors is shown in Fig. 2*C*) and performing assays of luciferase activity in LAN-5 and HEK-293 cells co-transfected with the *wt* or mutant reporters and with an expression vector for c-Myb or with the empty vector. As shown in Fig. 2*D*, mutation of site A lowered the c-Myb-induced increase in transcription activity of the Slug prom from 5.19- and 4.76- to 3.64- and 3.73-fold in HEK-293 and in LAN-5, respectively, compared with the activity of the corresponding promoter co-transfected with the empty vector. A similar decrease was caused by mutation in site B (4.40 and 3.51 in HEK-293 and LAN-5 respectively) and even more by the double mutation of sites A and B (3.44 and 3.25 in HEK-293 and LAN-5, respectively). The mut C reporter also had lower activity than the corresponding *wt* reporter (3.01 and 3.27-folds compared with 2.51- and 2.77-fold in HEK-293 and LAN-5 respectively), suggesting that c-Myb binding to the MBS in intron 1 is also relevant for transcription (Fig. 2*D*). In contrast, in the presence of c-Myb, the transcription activity of the mut D reporter was not significantly different from that of the corresponding *wt* reporter (Fig. 2*D*). Together, these data indicate that the *slug* gene contains MBS in the 5′-flanking region and in intron 1 important for c-Myb DNA binding-dependent transcription activity. It should be stressed that residual c-Myb-dependent transcription activity was detected in the assay with reporter plasmids mutated at sites A and/or B and in the first intron. To assess the relevance of endogenous c-Myb expression for transcription of the *slug* gene, K562 cells infected with the DOX-regulated pLVsh-c-Myb were transfected with reporter vectors containing the *wt* or the mutated forms of the *slug* regulatory regions, and luciferase activity was measured

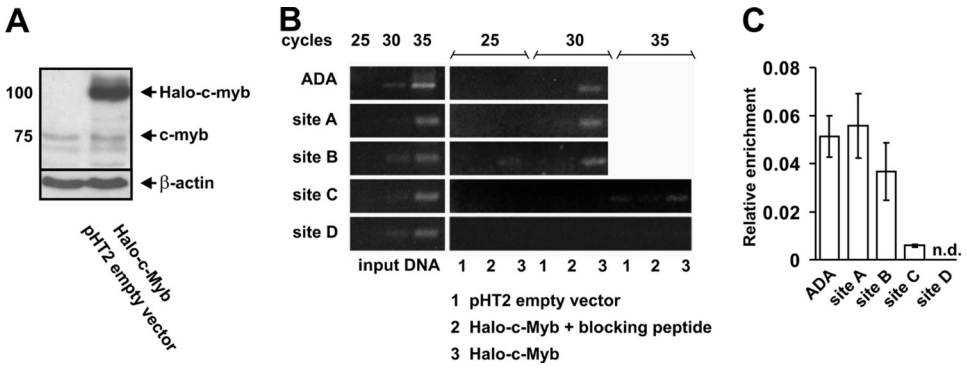

FIGURE 3. *A*, Western blot analysis to detect c-Myb in protein extracts from HEK-293 cells transfected with the Halo-c-Myb expression vector or the empty vector pHT2 is shown. *B*, ChIP was carried out in Halo-c-Myb-expressing HEK-293 cells. PCR analyses were carried out on immunoprecipitated DNA from Halo-c-Myb-transfected cells (*lanes 3*) with a set of primers designed to amplify regions containing sites A, B, C, and D in the *slug* gene and a MBS in the adenosine deaminase gene that was used as positive control. Each reaction was run for 25, 30, and 35 cycles (for sites C and D). Amplifications carried out with immunoprecipitated DNA from cells transfected with empty vector pHT2 (*lanes 1*) and with Halo-c-Myb and treated with the Halo-blocking peptide (*lanes 2*) were used as negative controls. The blots on the *left* show amplification of input DNA with each set of primers. *C*, ChIP was carried out in K562 cells. Immunoprecipitated DNA was analyzed by quantitative real-time PCR Data are expressed as relative enrichment ± S.D. (see "Experimental Procedures"). ChIP experiments were carried out twice with similar results. *ADA*, adenosine deaminase. *n.d.*, not determined.

after DOX treatment (7.5 μg/ml for 36 h). Consistent with the results of the luciferase assays in cells ectopically expressing c-Myb, down-regulation of endogenous c-Myb significantly reduced transcription from *slug* regulatory regions (Fig. 2*E*). Also in this setting, mutations in sites A and B (Slug prom) and in C (intron 1) affect c-Myb-dependent transcription, whereas mutation of site D in intron 2 is dispensable (Fig. 2*E*). Together, these studies support the importance of c-Myb expression in regulating transcription of the *slug* gene.

In Vivo Binding of c-Myb to MBS in the Promoter and in Intron 1 of the Slug Gene—To assess whether c-Myb interacts *in vivo* with the putative MBS identified in the regulatory regions of the *slug* gene, we performed ChIP assays in HEK-293 cells transfected with the pHT2-c-Myb-Halo expression plasmid. Halo-c-Myb expression in transfected cells was assessed by Western blot (Fig. 3*A*). After de-cross-linking, DNA was amplified by PCR using primers specific for segments including sites A, B, C, and D. As a positive control, we used a pair of primers that amplify a region that includes a MBS in the adenosine deaminase gene (30) validated for interaction with c-Myb in ChIP assays (31). After 30 PCR cycles, a clear band was detected using primers for sites A and B in the *slug* 5′ upstream region and for the adenosine deaminase gene-positive control (Fig. 3*B*). A faint band was visualized after 35 cycles using the primers for site C in intron 1. No amplification was detected utilizing the primers for site D in intron 2 even after 35 PCR cycles (Fig. 3*B*). Together, these data indicate that c-Myb efficiently binds *in vivo* to the 5′-regulatory region of the *slug* gene that includes sites A and B. Because these two putative MBSs are separated by 123 nucleotides, and the average size of sonicated DNA during the ChIP procedure was ~500 bp, we cannot determine whether the PCR amplification products obtained with the A and B sets of primers (Fig. 3*B*) reflected immunoprecipitated DNA fragments with c-Myb bound to site A or to site B or to both. In addition, our results indicate that c-Myb binds weakly to site C in intron 1. In contrast, site D in intron 2 does not appear to interact with c-Myb, at least in the experimental conditions utilized. Consistent with this, mutation of site D did not cause a change in transcriptional activity of the Slug intron 2 luciferase promoter (Fig. 2*D*). To assess whether endogenous c-Myb binds to the regulatory regions of the *slug* gene, we carried out ChIP assays in K562 cells that express high levels of c-Myb. Cross-linked DNA was immunoprecipitated with a c-Myb monoclonal antibody or with an unrelated antibody of the same IgG subclass or with no antibody. After de-cross-linking, immunoprecipitated DNA was amplified by quantitative real-time PCR. Amplification from anti-c-Myb-precipitated DNA was detectable for the regions including sites A, B, and C but not for site D (Fig. 3*C*). No significant amplification for any site was detectable using unrelated antibody- or no antibody-precipitated DNA (Fig. 3*C*). Thus, also endogenous c-Myb binds to sites A, B, and C but not to site D in the regulatory regions of the *slug* gene.

Slug Expression Driven by c-Myb Induces Lineage-specific Changes Consistent with an EMT Process and Increased Resistance to Apoptosis—To assess the functional significance of c-Myb regulation of Slug expression, HEK-293 embryonic kidney cells and LAN-5 neuroblastoma cells of epithelial and neuroectoderm origin, respectively (20), were transfected with c-Myb or with the pcDNA3 empty vector, and puromycin-resistant mixed cell populations were expanded and transduced with a pLKO lentiviral vector encoding the *slug* or GFP shRNA (control infection). c-Myb and Slug expression was assessed in each derivative cell line (pcDNA3/GFPkd, c-Myb/GFPkd, and c-Myb/Slugkd). As expected, c-Myb/GFPkd cells expressed higher levels of both c-Myb and Slug than the pcDNA3/GFPkd control cells (Fig. 4, *A* and *B*). Slug levels in c-Myb/Slugkd cells were lower than in c-Myb/GFPkd and in pcDNA3/GFPkd control cells (Fig. 4, *A* and *B*). Because c-Myb and Slug are involved in regulation of EMT (22, 32) and cell survival (33, 34), we analyzed the expression of genes involved in these processes. Compared with the pcDNA3/GFPkd control cells, Snail expression was unchanged in c-Myb/GFPkd and c-Myb/Slugkd HEK-293 and LAN-5 cells (Fig. 4, *A* and *B*). In contrast, vimentin and fibronectin expression slightly increased in c-Myb/GFPkd HEK-293 and LAN-5 cells compared with pcDNA3/GFPkd control cells, but it returned to the levels of control cells after Slug knockdown only in HEK-293 (see expression in c-Myb/Slugkd cells) (Fig. 4, *A* and *B*). Expression of pro-apoptotic Bax decreased in c-Myb/GFPkd HEK-293 and LAN-5 cells compared with pcDNA3/GFPkd control cells, but it increased after Slug knockdown in c-Myb/Slugkd cells (Fig. 4, *A* and *B*). Expression of anti-apoptotic Bcl-2 moderately increased in c-Myb/GFPkd LAN-5 cells as compared with pcDNA3/GFPkd control cells, and it returned to the levels of control cells in c-Myb/Slugkd transfected cells (Fig. 4, *A* and *B*). In HEK-293

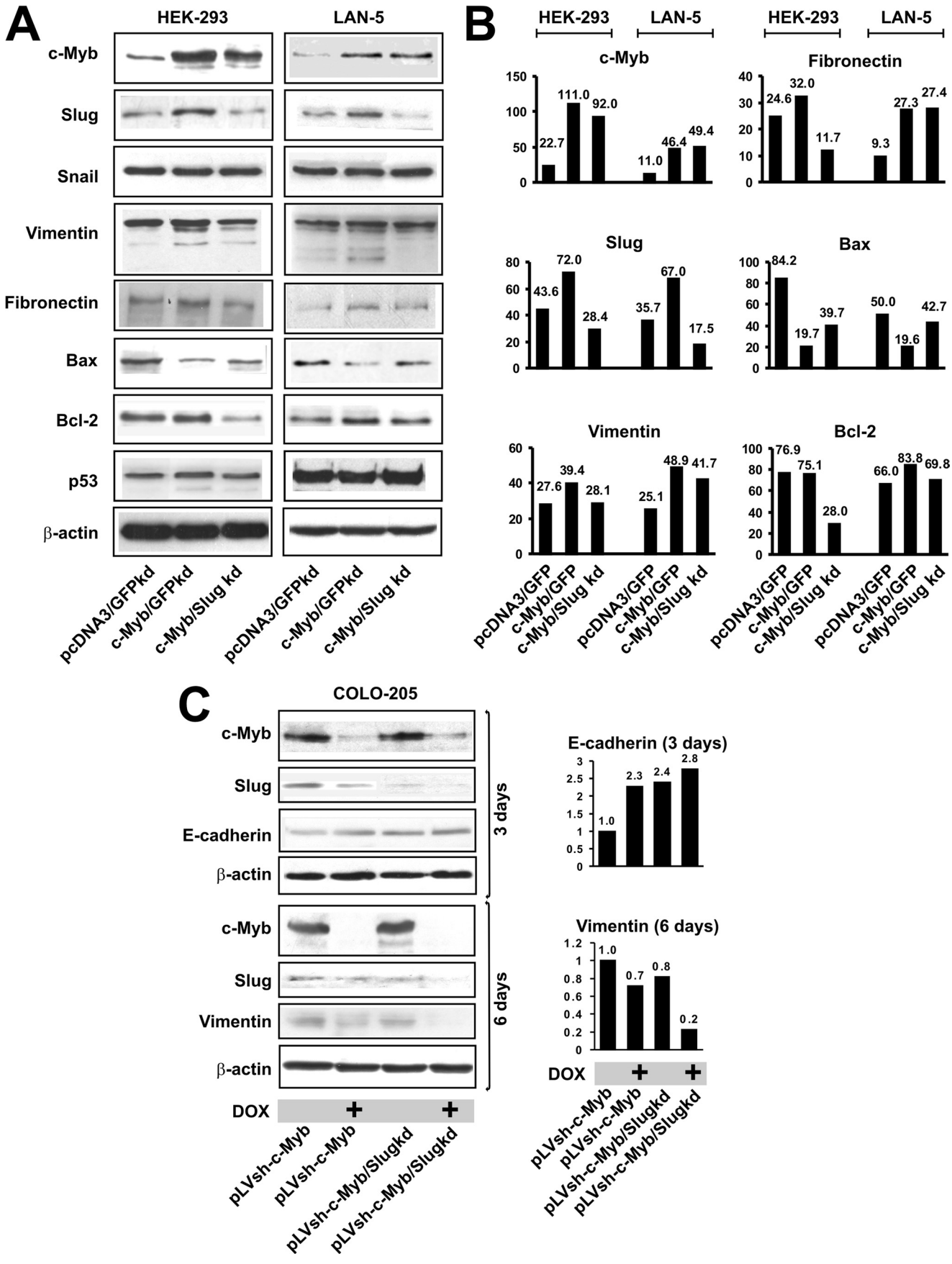
A
HEK-293
LAN-5
c-Myb
Slug
Snail
Vimentin
Fibronectin
Bax
Bcl-2
p53
β-actin
pcDNA3/GFPkd
c-Myb/GFPkd
c-Myb/Slug kd
pcDNA3/GFPkd
c-Myb/GFPkd
c-Myb/Slug kd
B
HEK-293
LAN-5
c-Myb
22.7
111.0
92.0
11.0
46.4
49.4
Fibronectin
24.6
32.0
11.7
9.3
27.3
27.4
Slug
43.6
72.0
28.4
35.7
67.0
17.5
Bax
84.2
19.7
39.7
50.0
19.6
42.7
Vimentin
27.6
39.4
28.1
25.1
48.9
41.7
Bcl-2
76.9
75.1
28.0
66.0
83.8
69.8
pcDNA3/GFP
c-Myb/GFP
c-Myb/Slug kd
C
COLO-205
c-Myb
Slug
E-cadherin
β-actin
3 days
c-Myb
Slug
Vimentin
β-actin
6 days
DOX
+
+
pLVsh-c-Myb
pLVsh-c-Myb
pLVsh-c-Myb/Slugkd
pLVsh-c-Myb/Slugkd
E-cadherin (3 days)
1.0
2.3
2.4
2.8
Vimentin (6 days)
1.0
0.7
0.8
0.2

TABLE 1

HEK-293 sensitivity to etoposide-induced apoptosis upon c-Myb overexpression alone or after Slug silencing

Statistical significance (p) was calculated by two-tailed Student's t test.

Cell treatments	Sub-G_1	p *vs.* pcDNA3/GFPkd	p *vs.* pcDNA3 c-myb/GFPkd
	%		
Untreated			
pcDNA3/GFPkd	4.90		
pcDNA3 c-myb/GFPkd	2.56	<0.0001	
pcDNA3 c-myb/Slugkd	7.27	<0.0001	<0.0001
1 day (etoposide 1 μM)			
pcDNA3/GFPkd	15.33		
pcDNA3 c-myb/GFPkd	8.54	<0.0001	
pcDNA3 c-myb/Slugkd	13.70	<0.0001	<0.0001
2 days (etoposide 1 μM)			
pcDNA3/GFPkd	33.34		
pcDNA3 c-myb/GFPkd	10.93	<0.0001	
pcDNA3 c-myb/Slugkd	17.35	<0.0001	<0.0001
3 days (etoposide 1 μM)			
pcDNA3/GFPkd	51.13		
pcDNA3 c-myb/GFPkd	15.82	< 0.0001	
pcDNA3 c-myb/Slugkd	22.60	< 0.0001	< 0.0001

cells, Bcl-2 levels did not increase after c-Myb transfection, but a significant decrease was observed after Slug knockdown (Fig. 4, *A* and *B*). Finally, levels of p53 were unchanged in all samples (Fig. 4*A*). Together, these results suggest that (i) c-Myb overexpression induces changes in gene expression that may affect apoptosis and cell morphology, and (ii) some of the detected changes are Slug-dependent. We also assessed whether levels of endogenous c-Myb could affect the expression of a prototypical epithelial marker such as E-cadherin and whether this effect was dependent on c-Myb-induced Slug expression. We used COLO-205 cells infected with pLVsh-c-Myb alone or with a constitutive vector encoding a shRNA directed against Slug (pLKO-Slug indicated as Slugkd). Cells were cultured in normal conditions or with DOX (7.5 μg/ml for 3 days). Expression of E-cadherin, a protein down-regulated during EMT (3), increased upon DOX treatment of pLVsh-c-Myb-transduced cells and in Slug-silenced cells (Fig. 4*C*). After 3 days of DOX treatment we did not detect any change in vimentin expression in pLVsh-c-Myb-transduced and in Slug-silenced cells (not shown), but a partial and yet significant decrease was detected after 6 days of c-Myb or Slug down-regulation (30 and 20%, respectively) (Fig. 4*C*). Simultaneous inhibition of c-Myb and Slug expression caused a more pronounced decrease of vimentin levels (80%) (Fig. 4*C*). These data support the role of c-Myb, in part through its control of Slug expression, in promoting phenotypic changes consistent with an EMT process. Finally, the mRNA levels of *desmoplakin* and *occludin*, two genes whose expression is high in epithelial cells and readily decreases upon mesenchymal differentiation (3), were measured by quantitative real-time PCR in COLO-205 cells infected with pLVsh-c-Myb. Upon c-Myb down-regulation induced by DOX treatment (7.5 μg/ml for 3 days), levels of *desmoplakin* and *occludin* mRNAs were significantly increased (supplemental Fig. S1).

c-Myb Expression Increases Apoptosis Resistance in HEK-293 Cells in Part through a Slug-dependent Mechanism—Apoptosis susceptibility of c-Myb/GFPkd (overexpressing c-Myb), c-Myb/Slugkd (overexpressing c-Myb and Slug-silenced), and pcDNA3/GFPkd (controls) HEK 293 cells was assessed after treatment with the chemotherapeutic drug etoposide. Cells were grown in the presence of 1 μM etoposide and at the indicated times (1, 2, and 3 days) were harvested, fixed in ethanol, and stained with propidium iodine for flow cytometric analysis of hypodiploid DNA content (Table 1). c-Myb/GFPkd HEK-293 cells were more resistant to etoposide-induced apoptosis than pcDNA3/GFPkd controls (8.54, 10.93, and 15.82 compared with 15.33, 33.34, and 51.13% of sub-G_1 cells after 1, 2, and 3 days of etoposide treatment). All these differences were highly significant (<0.0001, two-tailed Student's t test). Of interest, spontaneous apoptosis in untreated cells was also lower in Myb/GFPkd HEK-293 than in pcDNA3/GFPkd controls (2.56 *versus* 4.90% of sub-G_1 cells). The frequency of apoptotic cells was higher in c-Myb/Slugkd HEK-293 cells than in c-Myb/GFPkd HEK-293 cells (13.70, 17.35, and 22.60 compared with 8.54, 10.93, and 15.82% of sub-G_1 cells after 1, 2, and 3 days of etoposide treatment) but not as high as in pcDNA3/GFPkd control cells. Together, these data indicate that etoposide-induced apoptosis is blocked by c-Myb overexpression in HEK-293 cells, but the effect is only in part due to c-Myb-induced Slug up-regulation. Similar experiments carried out in LAN-5 cells overexpressing c-Myb (c-Myb/GFPkd) and after Slug silencing (c-Myb/Slugkd) failed to demonstrate significant changes of apoptosis after treatment with etoposide compared with controls (pcDNA3/GFPkd) (data not shown). However, it should be noted that after transfection with the c-Myb expression vector, c-Myb levels in LAN-5 were markedly lower than in HEK-293 cells (see blots in Fig. 4).

Motility and Invasion Changes Caused by c-Myb Overexpression—The changes in vimentin and fibronectin expression induced by modulation of c-Myb levels in various tumor lines (Fig. 4) are consistent with a mesenchymal-like phenotype often associated with increased migration and invasion capabilities (32). This was substantiated by immunofluorescence analysis to detect E- and N-cadherin expression and formation of F-actin fibers, which are associated with a motile phenotype (35). Levels of E-cadherin were not appreciably changed in c-Myb-overexpressing cells, and Slug knockdown did not affect E-cadherin levels in HEK-293 cells (Fig. 5, *A*–*C*), but it induced E-cadherin expression in LAN-5 cells (Fig. 5 compare *panel L* with *J* and *K*). Expression of N-cadherin was increased in c-Myb expressing HEK-293 and LAN-5 cells (Fig. 5, *E* and *N*). Of interest, N-cadherin expression was almost undetectable after Slug knockdown in HEK-293 (Fig. 5*F*) but not in LAN-5 cells (Fig. 5*O*). Detection of F-actin fibers showed membrane ruffling at

FIGURE 4. Shown are Western blot (*A*) and densitometry (*B*) analyses in HEK-293 and LAN-5 cells transfected with the pcDNA3 empty vector or the c-Myb expression vector and transduced with a lentiviral vector producing the shRNA against GFP (*pcDNA3/GFPkd* or *c-Myb/GFPkd* cells) or, in the case of c-Myb-transfected cells, with a lentiviral vector producing the shRNA against Slug (*c-Myb/Slugkd* cells). β-Actin was detected for normalization of protein extract loaded in each *lane*. *C*, shown are Western blot (*left*) and densitometry (*right*) analyses for c-Myb, Slug E-cadherin, and vimentin expression in untreated or DOX-treated COLO-205 cells infected with pLVsh-c-Myb or with pLVsh-c-Myb and pLKO-Slug. c-Myb, Slug, and E-cadherin were detected after 3 days, and vimentin was detected after 6 days of DOX treatment (7.5 μg/ml). β-Actin was detected for normalization.

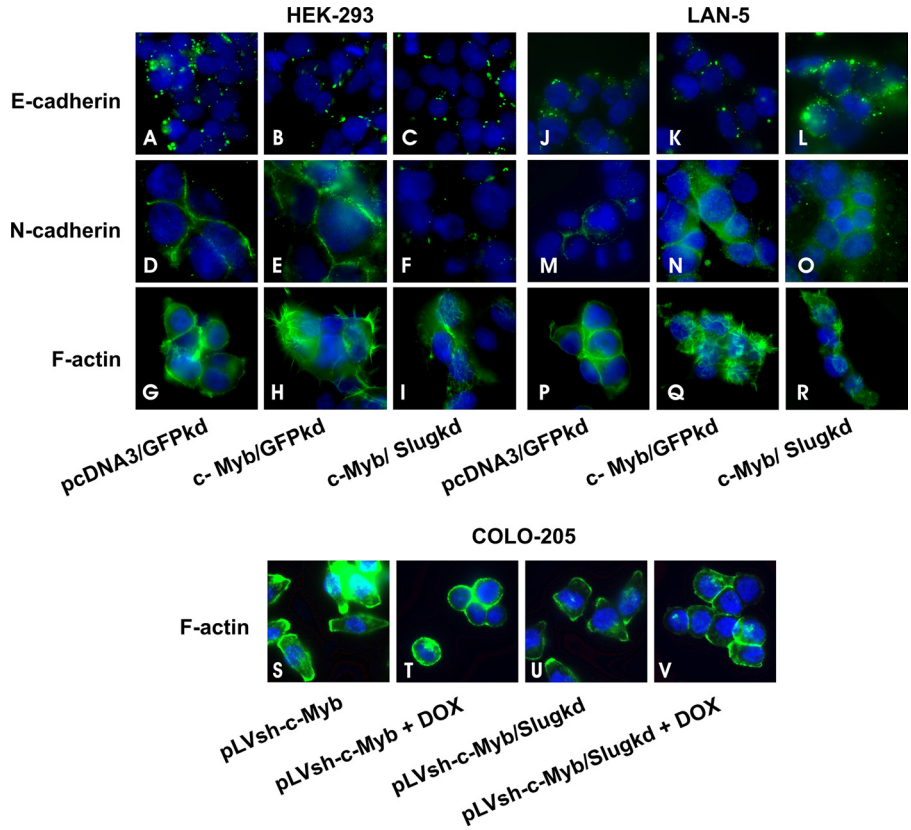

FIGURE 5. Shown is immunofluorescence detection of E-cadherin (*A–C* and *J–L*), N-cadherin (*D–F* and *M–O*), F-actin (*G–I* and *P–R*) in HEK-293 (*A–I*), and LAN-5 cells (*J–R*) transfected with the pcDNA3 empty vector and infected with a lentiviral vector producing the shRNA against GFP (*pcDNA3/GFPkd*) (*A*, *D*, *G*, and *J*, *M*, and *P*), the c-Myb expression vector and infected with a lentiviral vector producing the shRNA against GFP (*c-Myb/GFPkd*) (*B*, *E*, and *H* and *K*, *N*, and *Q*), and the c-Myb expression vector and infected with a lentiviral vector producing the shRNA against Slug (*c-Myb/Slugkd*) (*C*, *F*, and *I* and *L*, *O*, and *R*). *S*, *T*, *U*, and *V*, shown is immunofluorescence detection of F-actin in COLO-205 cells infected with pLVsh-c-Myb or with pLVsh-c-Myb and pLKO-Slug. DOX treatment was 7.5 μg/ml for 3 days. Original magnification was 100×. Nuclei were counterstained with DAPI.

the cell periphery in both HEK-293 and LAN-5 c-Myb-expressing cells (Fig. 5, *panels H* and *Q*). Membrane ruffling dimmed after Slug knock down (Fig. 5, *panels I* and *R*). Furthermore, we analyzed the expression of F-actin and the presence of stress fibers also in pLVsh-c-Myb COLO-205 cells after DOX-induced down-regulation of c-Myb and/or Slug knockdown in pLKO-Slug shRNA-transduced cells. Upon DOX treatment (7.5 μg/ml for 3 days), F-actin levels decreased, and cell morphology became more rounded (Fig. 5, *panels S* and *T*). A similar effect was obtained upon Slug knock down (Fig. 5, *panel U*) and by simultaneous inhibition of c-Myb and Slug (Fig. 5, *panel V*). Although immunofluorescence analyses are qualitative, collectively these data further support the notion that c-Myb expression promotes changes consistently with a mesenchymal-like phenotype. Next, we carried out experiments directly aimed at evaluating motility and invasion *in vitro*. First, we utilized the wound healing assay (29) to qualitatively assess cellular motility. c-Myb/GFPkd, c-Myb/Slugkd, and pcDNA3/GFPkd HEK-293 cells were grown to con-

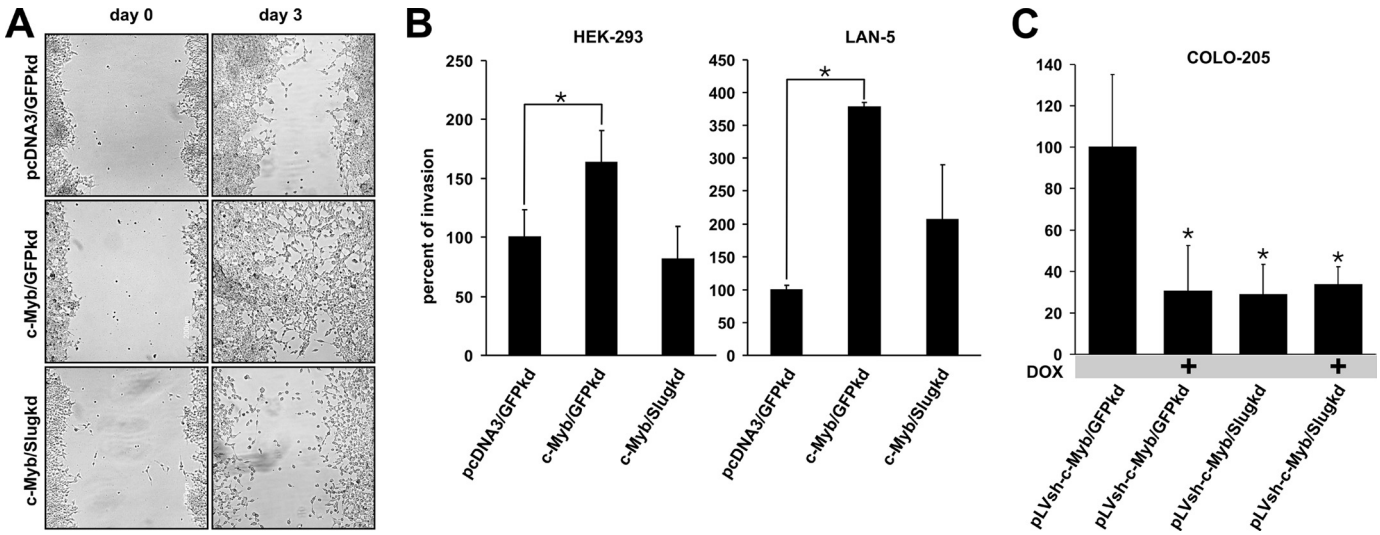

FIGURE 6. *A*, shown is a wound healing assay in HEK-293 cells transfected with the pcDNA3 empty vector and infected with a lentiviral vector producing the shRNA against GFP (*pcDNA3/GFPkd*), the c-Myb expression vector and infected with a lentiviral vector producing the shRNA against GFP (*c-Myb/GFPkd*), and the c-Myb expression vector and infected with a lentiviral vector producing shRNA against Slug (*c-Myb/Slugkd*). The same fields were photographed at day 0 and at day 3. *B*, invasion assays were carried out in HEK-293 and in LAN-5 cells using Matrigel-coated Boyden chambers. Transfection/infection combinations (indicated at the *bottom of the graphs*) are as in *A*. Values ± S.E. are reported. Percent of invasion was arbitrarily set at 100 for pcDNA3/GFPkd HEK-293 and LAN-5 cells. *C*, invasion assays using Matrigel-coated Boyden chambers in COLO-205 infected with pLVsh-c-Myb and with pLVsh-c-Myb and pLKO-Slug. Values ± S.E. are reported. Experiments in *B* and *C* were repeated twice in triplicate. *Asterisks* indicate statistical significance ($p < 0.05$, two-tailed Student's *t* test).

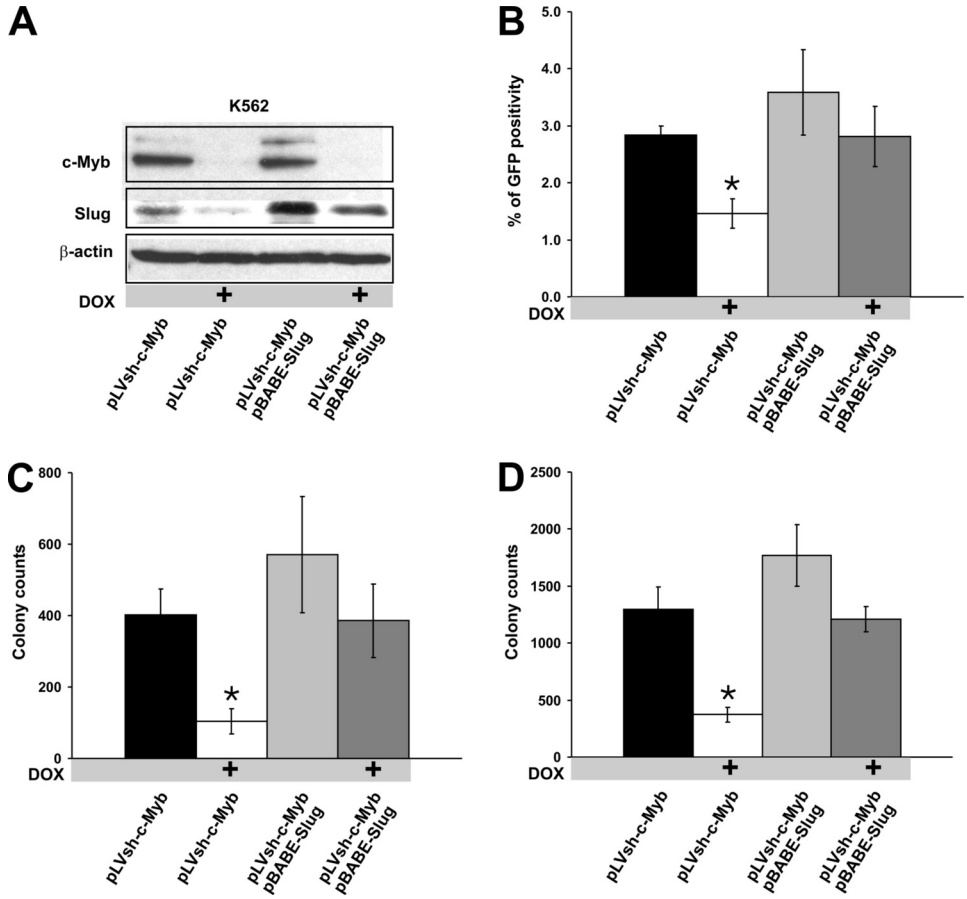

FIGURE 7. **Bone marrow homing of K562 cells is dependent on c-Myb-induced Slug.** *A*, shown is Western blot analysis for c-Myb and Slug expression in untreated or DOX-treated (36 h) K562 cells infected with pLVsh-c-Myb or with pLVsh-c-Myb and pBABE-puro-Slug. Cell identity is indicated at the *bottom of the blot*. *B*, bone marrow homing is calculated as the percent of GFP-positive cells in the bone marrow of NOD/SCID mice ($n = 3$) 24 h after injection of 2.5×10^6 cells/mouse. *C* and *D*, colony formation assays were carried out by plating in methylcellulose medium 1×10^4 (*C*) or 5×10^4 (*D*) bone marrow cells. Colonies were counted 5 days after plating. Data (triplicate experiments) are reported as the mean ± S.D. *Asterisks* indicate statistical significance ($p < 0.05$, two-tailed Student's *t* test).

fluence on plastic dishes before scratching the cell surface using a pipette tip. After 3 days, cells were observed under the microscope. The scratch was almost completely filled by c-Myb/GFPkd HEK-293 cells (Fig. 6*A*). In contrast, after 3 days, control pcDNA3/GFPkd and c-Myb/Slugkd cells did not bridge the gap (Fig. 6*A*). We failed to carry out the wound healing assay with LAN-5 cells because of their tendency to detach from the plastic substrate once they reached confluence. Invasion was tested using Boyden chambers in which upper and lower chambers are separated by a porous membrane coated with extracellular matrix proteins (Matrigel®). In HEK-293 and in LAN-5 cells, invasion significantly increased ($p < 0.05$) in cells overexpressing c-Myb (c-Myb/GFPkd) compared with control pcDNA3/GFPkd and to Slug knockdown (c-Myb/Slugkd) cells (Fig. 6*B*). Of interest, invasion decreased at levels similar to those of controls in c-Myb/Slugkd cells (Fig. 6*B*), indicating that Slug expression plays an important role in invasion in both cell lines.

To investigate whether c-Myb-regulated Slug expression affects invasion *in vitro*, we used COLO-205 cells infected with pLVsh-c-Myb and with a constitutive vector encoding a shRNA directed against Slug (pLKO-Slug, indicated as Slugkd in Fig. 6*C*) or against GFP (pLKO-GFP, indicated as *GFPkd* in Fig. 6*C*). Cells were cultured in normal medium or pretreated for 1 day with DOX (7.5 μg/ml) before seeding on Boyden chambers for invasion assays. Invasion was significantly inhibited ($p < 0.05$, Student's *t* test) upon DOX treatment of c-Myb shRNA-transduced COLO-205 cells (Fig. 6*C*). Slug knockdown decreased invasion by a similar extent even in the presence of c-Myb expression (Fig. 6*C*), indicating that c-Myb regulates invasion of COLO-205 cells largely through Slug.

c-Myb Affects Bone Marrow Homing of K562 Cells via Slug—To investigate the role of c-Myb-regulated *Slug* in an *in vivo* process required for metastasis, we performed a bone marrow "homing" assay using untreated or DOX (7.5 μg/ml, 36 h)-treated pLVsh-c-Myb or pLVsh-c-Myb/full-length Slug K562 cells injected in the tail vein of SCID mice (2.5×10^6 cells/animal). c-Myb and Slug expression were detected by Western blot before cell injection (Fig. 7*A*). Twenty-four hours after injection mice were sacrificed, and "homing" of K562 cells to the bone marrow was evaluated by flow cytometry analysis of GFP-positive cells. Bone marrow homing of untreated K562 cells was 2.84% (±0.16) but was reduced to 1.46% (±0.26) after DOX-induced c-Myb down-regulation. This difference was statistically significant ($p = 0.002$, Student's *t* test) (Fig. 7*B*). Of interest, bone marrow homing was completely rescued in DOX-treated pLVsh-c-Myb K562 cells ectopically expressing Slug (2.81% ± 0.56) (Fig. 7*B*). K562 expressing endogenous c-Myb and ectopic Slug had a slightly higher (3.59% ± 0.75) bone marrow homing compared with cells expressing c-Myb only (Fig. 7*B*). Bone marrow homing of K562 cells was independently evaluated by methylcellulose colony formation assays in the absence of cytokines to allow only growth factor-independent colony formation of K562 cells. Thus, 10,000 and 50,000 marrow cells from each injected mouse were plated in methylcellulose, and colonies were scored 5 days later. Results of the colony assays were in agreement with the flow cytometric determination of GFP-positive cells in the bone marrow. Colony formation from bone marrow cells of mice injected with DOX-treated pLVsh-c-Myb K562 cells was markedly suppressed compared with that of untreated cells, and ectopic Slug expression rescued almost completely the negative effect on colony formation induced by c-Myb down-regulation (Fig. 7, *C* and *D*).

DISCUSSION

We show here that c-Myb activates the expression of the transcription repressor Slug in embryonic kidney, colon carcinoma, chronic myeloid leukemia, and neuroblastoma cells. During kidney development, mesenchymal cells are initially formed by EMT, and subsequently some of these cells undergo mesenchymal epithelial transition to form the epithelia of the pronephros, mesonephros, and metanephros (36). It has been recently shown that Snail genes are repressed during kidney differentiation and that they regulate cadherin-16 expression by repressing hepatocyte nuclear factor-1β (9). In adult life, Snail and Slug reactivation has been associated with renal fibrosis (9) and kidney carcinoma progression (10). Noteworthy, Slug rather than Snail is activated in kidney cancer cells, in agreement with the prominent role of Slug in renal EMT (10). Snail and Slug expression is activated via the TGF-β axis signaling (8, 32), although information is incomplete on the identity of activator(s) of Snail/Slug transcription. Our data suggest that c-Myb can be involved in the acquisition of the invasive phenotype of embryonic kidney, colon carcinoma, and neuroblastoma cells for its ability to enhance Slug expression. Accordingly, cells overexpressing c-Myb invade more efficiently through Matrigel® membranes in *in vitro* assays. Moreover, our data show that c-Myb-induced Slug expression is essential for bone marrow homing of chronic myeloid leukemia K562 cells in NOD/SCID mice. Furthermore, quantitative (Western blotting) and qualitative (immunofluorescence) data on vimentin, fibronectin, E-cadherin expression, and F-actin fibers formation suggest that cells overexpressing c-Myb acquire mesenchymal-like characteristics.

c-Myb overexpression in embryonic kidney cells causes an increase in resistance to etoposide-induced apoptosis. This process is largely Slug-dependent as tumor cells reacquire the sensitivity of parental cells after Slug silencing. In contrast with the results in HEK-293 cells, we did not observe protection from etoposide-induced apoptosis in LAN-5 cells overexpressing c-Myb. This discrepancy may be explained by the lower levels of c-Myb expressed in LAN-5 compared with HEK-293, although we cannot rule out cell type-specific differences. Thus, the effects of c-Myb-induced Slug on apoptosis protection need further characterization by using additional cell types and detection methods.

Of interest, in birds, c-Myb is able to promote EMT in neural crest cells activating the expression of *msx-1* and *slug* mRNAs (22), supporting the notion that c-Myb function goes beyond its role as a key regulator of hematopoiesis. We show here that c-Myb expression bestows mesenchymal features (increase of vimentin and fibronectin, membrane ruffling via F-actin polymerization at the cell periphery) to neuroblastoma cells and increases their invasion capability. Some of these changes were not detected in neuroblastoma (LAN-5) and in embryonic kidney cells (HEK-293). These discrepancies are likely due to the different origin of these cells. In neuroblastoma cells, the observed changes, reminiscent of delaminating neuroblasts in the embryo, are mostly dependent on c-Myb-induced Slug activation as demonstrated by the rescue of the phenotype of parental cells after silencing Slug expression.

c-Myb is not alone among oncogenes in playing a role in neural crest formation. The proto-oncogene c-Myc is an essential early regulator of neural crest cell formation in *Xenopus* (37). Of interest, c-Myc is localized at the neural plate border before the expression of early neural crest markers, such as Slug (37). In the avian neural crest, c-Myb expression is activated by bone morphogenic protein 4 (BMP4), a cytokine that plays a central role in determining the fate of embryonic neuroectodermal cells (38). It is now widely recognized that several growth factors and cytokines act in the acquisition of the invasive phenotype of many tumors (39). Thus, it is conceivable that in neuroblastoma, a tumor of neural crest origin (40), cancer cells increase their motility by growth factor- or cytokine-mediated signaling, which activates the expression of c-Myb that, in turn, induces Slug expression.

A possible role of c-Myb in metastasis has been suggested in colon cancer by its ability to activate acetylcholinesterase that in turn promotes anchorage-independent growth (41). When inappropriately expressed, as in leukemia and epithelial cancers of the breast, colon, and gastro-esophagus, c-Myb appears to activate gene targets of key importance for cancer progression and metastasis (42). Thus, our observation that c-Myb activates Slug expression not only in neuroblastoma and embryonic kidney cells but also in colon carcinoma and in chronic myeloid leukemia-blast crisis cells, is consistent with a broad role of c-Myb in tumor invasion.

In colon cancer cells (COLO-205), down-regulation of c-Myb and/or Slug expression led to increased E-cadherin, *desmoplakin*, and *occludin*, and decreased Vimentin expression and reduced invasion capability, indicating that the connection between c-Myb and Slug is important in regulating the invasive phenotype of tumors of different origin. In agreement with these data, we also demonstrated that c-Myb induced Slug expression is central for bone marrow homing of K562 cells in SCID mice. To our knowledge this is the first indication of a functional role of Slug in leukemic cells.

The role of c-Myb in controlling Slug expression is exerted through a transcriptional, partly DNA binding-dependent, mechanism as shown in HEK-293 cells ectopically expressing c-Myb and upon down-regulation of endogenous c-Myb in K562 cells. We mapped four potential MBS, two located in the 5′ region of the gene and the remaining two in intron 1 and intron 2. The latter does not bind c-Myb in ChIP experiments, although intron 2 possesses c-Myb-dependent enhancer activity in functional assays. This suggests that c-Myb can exert transcriptional control on Slug also by indirect mechanisms such as induction of other transcription factors or inhibition of repressor(s) that act directly on intron 2. Nevertheless, the enhancer activity of intron 2 may derive from the presence of three additional MBS, detected with transcription factor search, that were not included in our analysis because their homology to the MBS consensus was lower than the utilized threshold (86%). These MBS in intron 2 can be low affinity sites for c-Myb that, although able to function as transcription enhancers in luciferase assays, were not bound by c-Myb in ChIP experiments. The MBS in intron 1 shows very weak binding in ChIP experiments, leaving the two sites in the 5′-regulatory region as the main c-Myb binding-dependent enhancer elements. We have previ-

ously demonstrated that c-Myb exerts transcriptional control on IGFBP-5, a member of the IGF axis, through direct and indirect mechanisms in neuroblastoma cells (27). Thus, the presence of c-Myb sensitive, binding-independent sequences in the introns of Slug would be consistent with the possibility that c-Myb cooperates with other transcription factors or by mechanisms that do not require direct binding to DNA. Furthermore, the residual c-Myb-dependent transcription activity detected with luciferase plasmids carrying mutations in the 5′-regulatory region MBS is in agreement with a DNA binding-independent role of c-Myb, although we cannot rule out the possibility that the mutations decreased but did not abolish c-Myb binding.

c-Myb-dependent regulation of *slug* gene expression occurs similarly in cells as diverse as embryonic kidney, colon carcinoma, chronic myeloid leukemia, and neuroblastoma. Of interest, *twist-1* expression is associated with MYCN amplification, advanced (metastatic) stage and poor outcome in neuroblastoma patients (43). These data and our present work suggest a scenario in which two oncoproteins (MYCN and c-Myb) expressed in neuroblastoma control at the transcription level the expression of two invasion-associated genes (*twist-1* and *slug*) in a network that contributes to the acquisition of the invasive phenotype.

In summary, we have identified c-Myb as a new transcriptional regulator of *slug*. c-Myb-dependent changes in migration/invasion capabilities, bone marrow homing, and resistance to drug-induced apoptosis support its critical role in part via transcriptional regulation of Slug expression in tumors of different origin.

Acknowledgments—We greatly appreciate the skillful technical assistance of Camillo Mancini. We thank Dr. T. J. Gonda for the generous gift of lentiviral vector pLVsh-c-Myb and Dr. G. Starace for cell sorting.

REFERENCES

1. Liotta, L. A. (2001) *Nature* **410,** 24–25
2. Steeg, P. S. (2006) *Nat. Med.* **12,** 895–904
3. Thiery, J. P., and Sleeman, J. P. (2006) *Nat. Rev. Mol. Cell Biol.* **7,** 131–142
4. Peinado, H., Olmeda, D., and Cano, A. (2007) *Nat. Rev. Cancer* **7,** 415–428
5. Yang, J., and Weinberg, R. A. (2008) *Dev. Cell* **14,** 818–829
6. Hartwell, K. A., Muir, B., Reinhardt, F., Carpenter, A. E., Sgroi, D. C., and Weinberg, R. A. (2006) *Proc. Natl. Acad. Sci. U.S.A.* **103,** 18969–18974
7. Gilmore, A. P. (2005) *Cell Death Differ.* **12,** 1473–1477
8. Barrallo-Gimeno, A., and Nieto, M. A. (2005) *Development* **132,** 3151–3161
9. Boutet, A., De Frutos, C. A., Maxwell, P. H., Mayol, M. J., Romero, J., and Nieto, M. A. (2006) *EMBO J.* **25,** 5603–5613
10. Boutet, A., Esteban, M. A., Maxwell, P. H., and Nieto, M. A. (2007) *Cell Cycle* **6,** 638–642
11. Gupta, P. B., Kuperwasser, C., Brunet, J. P., Ramaswamy, S., Kuo, W. L., Gray, J. W., Naber, S. P., and Weinberg, R. A. (2005) *Nat. Genet.* **37,** 1047–1054
12. Catalano, A., Rodilossi, S., Rippo, M. R., Caprari, P., and Procopio, A. (2004) *J. Biol. Chem.* **279,** 46706–46714
13. Vitali, R., Mancini, C., Cesi, V., Tanno, B., Mancuso, M., Bossi, G., Zhang, Y., Martinez, R. V., Calabretta, B., Dominici, C., and Raschellà, G. (2008) *Clin. Cancer Res.* **14,** 4622–4630
14. Olmeda, D., Montes, A., Moreno-Bueno, G., Flores, J. M., Portillo, F., and Cano, A. (2008) *Oncogene* **27,** 4690–4701
15. Ramsay, R. G., and Gonda, T. J. (2008) *Nat. Rev. Cancer* **8,** 523–534
16. Melani, C., Rivoltini, L., Parmiani, G., Calabretta, B., and Colombo, M. P. (1991) *Cancer Res.* **51,** 2897–2901
17. Ramsay, R. G., Thompson, M. A., Hayman, J. A., Reid, G., Gonda, T. J., and Whitehead, R. H. (1992) *Cell Growth Differ.* **3,** 723–730
18. Guérin, M., Sheng, Z. M., Andrieu, N., and Riou, G. (1990) *Oncogene* **5,** 131–135
19. Kauraniemi, P., Hedenfalk, I., Persson, K., Duggan, D. J., Tanner, M., Johannsson, O., Olsson, H., Trent, J. M., Isola, J., and Borg, A. (2000) *Cancer Res.* **60,** 5323–5328
20. Raschellà, G., Negroni, A., Skorski, T., Pucci, S., Nieborowska-Skorska, M., Romeo, A., and Calabretta, B. (1992) *Cancer Res.* **52,** 4221–4226
21. Raschellà, G., Cesi, V., Amendola, R., Negroni, A., Tanno, B., Altavista, P., Tonini, G. P., De, Bernardi, B., and Calabretta, B. (1999) *Cancer Res.* **59,** 3365–3368
22. Karafiat, V., Dvorakova, M., Krejci, E., Kralova, J., Pajer, P., Snajdr, P., Mandikova, S., Bartunek, P., Grim, M., and Dvorak, M. (2005) *Cell. Mol. Life Sci.* **62,** 2516–2525
23. Graham, F. L., Smiley, J., Russell, W. C., and Nairn, R. (1977) *J. Gen. Virol.* **36,** 59–74
24. Drewinko, B., Yang, L. Y., Barlogie, B., Romsdahl, M., Meistrich, M., Malahy, M. A., and Giovanella, B. (1978) *J. Natl. Cancer Inst.* **61,** 75–83
25. Ratajczak, M. Z., Kant, J. A., Luger, S. M., Hijiya, N., Zhang, J., Zon, G., and Gewirtz, A. M. (1992) *Proc. Natl. Acad. Sci. U.S.A.* **89,** 11823–11827
26. Drabsch, Y., Hugo, H., Zhang, R., Dowhan, D. H., Miao, Y. R., Gewirtz, A. M., Barry, S. C., Ramsay, R. G., and Gonda, T. J. (2007) *Proc. Natl. Acad. Sci. U.S.A.* **104,** 13762–13767
27. Tanno, B., Negroni, A., Vitali, R., Pirozzoli, M. C., Cesi, V., Mancini, C., Calabretta, B., and Raschellà, G. (2002) *J. Biol. Chem.* **277,** 23172–23180
28. Gurtner, A., Starace, G., Norelli, G., Piaggio, G., Sacchi, A., and Bossi, G. (2010) *J. Biol. Chem.* **285,** 14160–14169
29. Savagner, P., Kusewitt, D. F., Carver, E. A., Magnino, F., Choi, C., Gridley, T., and Hudson, L. G. (2005) *J. Cell. Physiol.* **202,** 858–866
30. Ess, K. C., Whitaker, T. L., Cost, G. J., Witte, D. P., Hutton, J. J., and Aronow, B. J. (1995) *Mol. Cell. Biol.* **15,** 5707–5715
31. Berge, T., Matre, V., Brendeford, E. M., Saether, T., Lüscher, B., and Gabrielsen, O. S. (2007) *Blood Cells Mol. Dis.* **39,** 278–286
32. Nieto, M. A. (2009) *Int. J. Dev. Biol.* **53,** 1541–1547
33. Inukai, T., Inoue, A., Kurosawa, H., Goi, K., Shinjyo, T., Ozawa, K., Mao, M., Inaba, T., and Look, A. T. (1999) *Mol. Cell* **4,** 343–352
34. Thompson, M. A., Rosenthal, M. A., Ellis, S. L., Friend, A. J., Zorbas, M. I., Whitehead, R. H., and Ramsay, R. G. (1998) *Cancer Res.* **58,** 5168–5175
35. Yilmaz, M., and Christofori, G. (2009) *Cancer Metastasis Rev.* **28,** 15–33
36. Dressler, G. R. (2002) in *Mouse Development* (Rossant, Ja. T. P. T., ed) pp. 395–420, Academic Press, Inc., San Diego, CA
37. Bellmeyer, A., Krase, J., Lindgren, J., and LaBonne, C. (2003) *Dev. Cell* **4,** 827–839
38. Liem, K. F., Jr., Tremml, G., Roelink, H., and Jessell, T. M. (1995) *Cell* **82,** 969–979
39. Civenni, G., and Sommer, L. (2009) *Semin. Cancer Biol.* **19,** 68–75
40. Brodeur, G. M. (2003) *Nat. Rev. Cancer* **3,** 203–216
41. Syed, M., Fenoglio-Preiser, C., Skau, K. A., and Weber, G. F. (2008) *Clin. Exp. Metastasis* **25,** 787–798
42. Ramsay, R. G., Barton, A. L., and Gonda, T. J. (2003) *Expert Opin. Ther. Targets* **7,** 235–248
43. Valsesia-Wittmann, S., Magdeleine, M., Dupasquier, S., Garin, E., Jallas, A. C., Combaret, V., Krause, A., Leissner, P., and Puisieux, A. (2004) *Cancer Cell* **6,** 625–630